World Academy of Science, Engineering and Technology
International Journal of Computer and Systems Engineering
Vol:17, No:6, 2023

Offset Dependent Uniform Delay Mathematical Optimization Model for Signalized Traffic Network Using Differential Evolution Algorithm

Tahseen Al-Shaikhli, Halim Ceylan, Jonathan Weaver, Osman Nuri Çelik, Onur Gungor Sahin

***Abstract*—**A concept of uniform delay offset dependent mathematical optimization problem is derived as the main objective for this study using a differential evolution algorithm. Furthermore, the objectives are to control the coordination problem which mainly depends on offset selection, and to estimate the uniform delay based on the offset choice at each signalized intersection. The assumption is the periodic sinusoidal function for arrival and departure patterns. The cycle time is optimized at the entry links and the optimized value is used in the non-entry links as a common cycle time. The offset optimization algorithm is used to calculate the uniform delay at each link. The results are illustrated by using a case study and compared with the canonical uniform delay model derived by Webster and the highway capacity manual's model. The findings show that the derived model minimizes the total uniform delay to almost half compared to conventional models; the mathematical objective function is robust; the algorithm convergence time is fast.

***Keywords*—**Area traffic control, differential evolution, offset variable, sinusoidal periodic function, traffic flow, uniform delay.

I. Introduction

THE mathematical relationship of the delay-offset variable is needed to provide the uniform delay to be offset dependent as the main objective of this study. Generally, the total delay is divided into two components uniform and oversaturated as it was exploded in the canonical delay expressions by [1]. In this paper, the uniform delay is the first Webster's expression term and the Highway Capacity Manual (HCM) uniform delay model is investigated. Delay in a signalized traffic network was extensively studied by [1]-[3]. However, the coordination parameter choice could lead to total delay minimization under area traffic control when the performance index function is weighted by the delay parameter and stops [4]-[9]. The first expression of uniform delay needed to be linked with the offset variable to address the problem. This study focuses on a direct mathematical formulation of a delay-offset function based on offset optimization to achieve a minimum uniform delay component with realistic coordination in a signalized traffic network. In addition, the robustness of the HCM model and Webster's first term delay expression has been studied, considered, and evaluated in many research papers [10]-[14], although the model has no direct relationship with the coordination parameters. A branch-and-backtrack method was used to solve the combination method aiming to relax the convexity estimation of the delay-offset function [15]. The Equilibrium Network Traffic Signal setting problem was investigated to improve the coordination of the traffic movements in urban networks by using a mixed-binary programming technique [16]. Cost function of [16] uses the link delay-offset function and Webster's model is calculated at each iteration thereby the offset selection choice is made by the minimum delay calculated for a specific link.

The arrival rate pattern represents the demand in the signalized network. The uniform delay model was derived by Webster to simulate the uniform delay that relays on the Poisson arrivals rate [1]. The area formed between the two lines is seen to be triangular, and this area is known as Webster's delay parameter. A consideration of the traffic demand (arrival flow) to be cyclic and periodically identical while the service rate was represented by a constant saturated flow [17]. The study [17] also used the area formed between the demand (arrival flow) and service (departure flow) which is not a uniform shape and represents the delay (Vehicle-hour/hour). Reference [18] presented the IN and GO patterns of a queue at each cycle and these patterns represent the accumulated arrival and departure rates per cycle. The uniform delay is the area formed bounded between the arrivals and departures curves. A polygon area formed by the arrivals and departures curves is represented by the queue length. It was indicated by term called incremental queue accumulation (IQA) with number of queued vehicles as a function of time and the control delay is measured proposed by [19]. The queue fluid model is presented to the traffic signal problem with demand (arrivals) and service (departure) assumed to be periodic sinusoidal functions [20]-[25].

Queue length is a critical parameter when total delay, traffic timing, performance index (combination of delay and stops), and offset optimization are presented to the signal optimization problem. Based on the literature, the queue length has been studied by two groups. In the first group, the average queue length is measured mathematically excluding the offset variable

T. A. Al-Shaikhli is with the Selcuk University, Civil Engineering Department, Konya, 42130 Turkey (corresponding author, phone: +964-7731200274; e-mail: tahseensaad@gmail.com).

H. Ceylan is with Pamukkale University, Department of Civil Engineering, Denizli, 20017 Turkey (e-mail: halimc@pau.edu.tr).

J. Weaver is with the Mechanical Engineering Department, University of Detroit Mercy, Detroit, W 4001 USA, (e-mail: weaverjm@udmercy.edu).

ON. Çelik is with Faculty of Engineering, Department of Civil Engineering, Konya Technical University, Konya, 42250 Turkey, (e-mail: oncelik@ktun.edu.tr).

SA. Onur is with Department of International Water Resources, Izmir Institute of Technology. 35433 Izmir, Turkey, (e-mail: onursahin@iyte.edu.tr).

effect for a signalized traffic network [19], [26], [27]. In the second group, the offset variable is included directly with a mathematical expression as the main variable to be optimized to minimize the average queue length and then minimize the total delay value in large-scale networks [20]-[25]. The second group has successfully optimized the queue length by using a convex optimization technique. However, since the queue length is a critical parameter for total delay minimization, it is considered as a host attribute between the offset variable and delay parameter, although it is possible to drive a direct mathematical relationship between the offset variable and delay in the signalized traffic network.

The optimization methods used in traffic signal timing are varied based on the problem type and variables included in the problem. As the signalized traffic problem is non-convex, researchers tested the efficiency of some algorithms such as the genetic algorithm [5], [9], [28], and showed the ability of such algorithms to handle the non-convexity correlation among traffic parameters, although the methods are computationally intensive. Reference [29] applied the cell-transmission model (CTM) adopted with the help of heuristic optimization algorithms such as genetic algorithm (GA) to trace the optimal offset variable for the urban network. The hill-climbing algorithm is adapted by [27] for the TRANSYT traffic program results with satisfactory results. Reference [5] developed a TRANSYT protocol to solve the area traffic control problem by combining the GA with the hill-climbing algorithm; the methods produced from this combination, namely the ADESS and GATHIC, showed that GATHIC is better than TRANSYT when applied to the traffic signal problem. Reference [30] evaluated the five most frequently used algorithms: hill-climbing, combination method formulation, quasi-exhaustive search, Monti Carlo selection, and GA to optimize the offset variable. Results of [30] show that the first, the second, and the last algorithms produce a comparable result and converge to the optimal solution faster than the other two. The second group we mentioned in the previous paragraph to optimize the offset variable depends on convex optimization problems using quadratic constraint quadratic problem (QCQP) as in [21] and [25]. A study that applied a binary-mixed-Integer-Linear-Programming model adopted by [12]-[26] showed that the optimization method is effective at finding the optimal solution in both offset optimization in traffic signal networks and in optimization of the cycle time in the isolated signalized intersection. Since the GA converges to an optimal solution as indicated above, the differential evolution (DE) optimization algorithm is proposed by [31] to solve the equilibrium network design (EQND) problem. The DE algorithm is a further developed version of the GA; this metaheuristic approach was found by [32]. The DE can be used when minimizing possibly nonlinear and non-differentiable continuous space functions. The estimation of average delay is investigated by comparing the results of two metaheuristics algorithms: genetic and DE [33]. In addition, the study shows that the DE algorithm presents the best convergence rate.

In this paper, we drive a direct mathematical relationship between the offset variable and uniform delay component to solve the synchronization problem and minimize the uniform delay. This study also connects the previous concepts purposed by [1] for the uniform delay that is subject to the triangular area formed between the arrivals and departure under Poisson's distribution to the recent concept presented by [21]-[25] which considers the arrivals and departure rates to be sinusoidal periodic functions. The uniform delay is the difference between areas bounded between the arrival and departure sinusoidal functions under the red interval and the green interval. These functions are manipulated to suit the goal of this study, namely estimating and minimizing the uniform delay. In addition, the DE algorithm is used to solve the non-convex delay-offset objective function.

The delay-offset objective function is applied to an academic case study of 23 links, divided in such manner of seven entry links and 16 non-entry links with nine signalized intersections [34] and the results are compared with Webster's uniform delay and HCM model. Based on the optimization DE algorithm, this shows the robustness of objective function compared with previous uniform delay models. Finally, the DE algorithm efficiently converges to a solution with less time compared to other mathematical objective functions and metaheuristic algorithms used by [5], [9], [28], [31].

II. Problem Formulation

The uniform delay is estimated in terms of sinusoidal periodic functions which is represented by area bounded between arrival and departure rates. The uniform delay formula for the periodic function is given. Webster proposed the triangular area formed between arrival curve and departure curve at signalized intersection. The area of triangle represents the uniform delay in signalized intersection; the concept is the same but the area here is formed between two sinusoidal periodic functions. The optimization techniques are carried out to minimize the uniform delay component.

The uniform delay model is formulated by considering the differences in the area bounded between the periodic sinusoidal arrivals and departure rate functions under red and green intervals. However, in this study, it is the difference between the areas bounded in green and red intervals.

As was revealed in the introduction, researchers adopted the fluid queue model to simulate the queue length at signalized traffic networks [21], [22], [25]. The traffic demand may not be the same for all links. The model is derived in such a case that it can be applied by real-time data measurements from the field (out of the scope of the study). At each entry link l, arrival and departure rates, offsets at up and downstream, and green splits are analyzed. The parameter notations used within this work are presented in Table I.

To determine the relationship between delay parameter and offset variable, this work adopts the traffic network model with sinusoidal approximation by [21], [25]. In what follows, we will first describe the model and explain this sinusoidal approximation technique. Then, using this model, we formulate a mathematical optimization problem to select an offset that minimizes the uniform delay under saturation conditions for the

network. Fig. 1 illustrates the simple network under study.

TABLE I
SETS, SUBSETS, VARIABLE AND PARAMETERS NOTATIONS

Sets	Description
G	is a graph containing nodes and edges $(W \cup \{\epsilon\}, \mathcal{L})$
W	is the set of all nodes $i \in W = \{1,2, \dots, \lvert W \rvert\}$
$\mathcal{L}$	is the set of all links
$\mathcal{E}$	is the set of all entry links $\{l \in \mathcal{L}, \tau(l) = \epsilon\} \subset \mathcal{L}$
	Indices
$\tau(l)$	is the upstream intersection $\in W$
$\sigma(l)$	is the downstream intersection $\in W$
l	is the entry links that links the upstream and downstream intersections $= 1, 2, \dots k$
w	is a node in the grid network w $\in W = 1, 2, \dots n$
	Parameters
C	is the cycle length (sec)
g	is the effective green time (sec)
r	is the effective red time (sec)
Q_l	is the capacity of link l (veh/h)
s_l	is the saturation flow rate at link l (veh/h)
q_l	is the flow at link l (veh/h)
x_l	is the saturated degree for link l
Cycle time	$C = 1$
Offset of w $\in W$	$\theta_w \in [0,1)$
φ_l	$\varphi_l \in [0,1)$ is the offset at the center of the peak arrival rate
Traffic demand at link l	is the volume of traffic requesting a trip at an entry link l to a signalized intersection
Green split	$\gamma_l \in [0,1)$ is the time difference of the midpoint of the activation time for the link and the beginning of the offset time at $\sigma(l)$. $n + \theta_{\sigma(l)} + \gamma_l \; for \; n = 0,1 \dots$ Green split can also be defined as the ratio of the traffic demand between link $l \; and \; k$. It can also be the ratio of the effective green of the whole cycle length $\gamma_l = \frac{g}{C}$
Activation offset	$\theta_{\sigma(l)} + \gamma_l$
A_l	$\exp(-i2\pi\varphi_l)$ is the offset at the peak arrival rate
D_l	$\exp(-i2\pi\gamma_l)$is the green split at the downstream intersection
$z_{\tau(l)}$	$\exp(-i2\pi\theta_{\tau(l)})$ is the offset at the upstream intersection
$z_{\sigma(l)}$	$\exp(-i2\pi\theta_{\sigma(l)})$ is the offset at the downstream intersection
P	$\exp\left(-i \arctan\left(\frac{\alpha_l A_l z_{\tau(l)} - f_l D_l z_{\sigma(l)}}{B_l D_l z_{\sigma(l)} - \alpha_l A_l B_l z_{\tau(l)}}\right)\right)$ is the arctangent to estimate the delay at each intersection S. $P \in [0, \frac{\pi}{2}]$
UD_l	The estimated uniform delay at link l
OD_l	The estimated oversaturated delay at link l
TD_l	The estimated total delay at link l (veh-h/h)
m_l	the slop variable for the linear part for the arrival rate at link l
f_l	is the average number of arrival rate at link l $f_l \geq \alpha_l$
d_l	is the average number of departure rate at link l
α_l	is the fluctuation in the arrival rate at link l
B_l	$f_l \exp(-\pi i/2)$ is constant

Let's consider a simple traffic network as shown in Fig. 1. $G = (W \cup \{\epsilon\}, \mathcal{L})$. The signalized intersections are represented by nodes; node $i \in W = \{1,2,3, \dots, \lvert W \rvert\}$ represents a set of signalized intersection and node ϵ is the dummy intersection (source) for traffic originating outside the network. Let $n = \lvert W \rvert + 1$ be the number of intersections including the dummy intersection. The dummy node ϵ is also referred to as node n. Each directed edge in $\mathcal{L}$ represents a traffic link between two intersections signals and the vehicle queue associated with the link. For each $\epsilon \in \mathcal{L}, \sigma(\epsilon)$ indicates the downstream intersection for the entry (dummy) links because it is controlled by a traffic light. Thereby $\sigma(\epsilon) = \tau(l)$, for each $\iota \in L, \tau(\iota) \in W$ indicates its upstream intersection where vehicles enter the network and $\sigma(\iota) \in W$ represents the downstream intersection which discharges the queue of the link. $\mathcal{E} = \{\epsilon \in \mathcal{L}, l \in \mathcal{L}, \tau(\iota) = \epsilon, \sigma(\epsilon) = l\} \subset \mathcal{L}$ is the set of entry links that directed exogenous traffic from the dummy intersection (source) to the network; other links are non-entry links and the travel time from its upstream to downstream intersections is denoted by λ_l. There is no need to explicitly model links that exist in the network because exiting traffic is considered in the calculation of the turning ratio, which will be explained later.

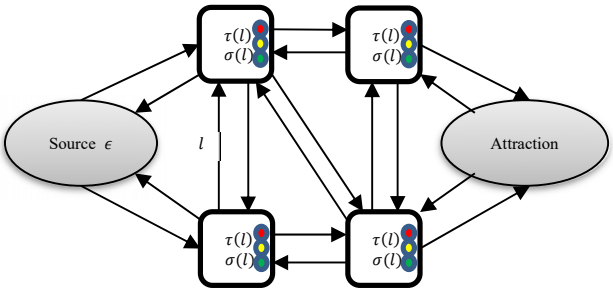

Fig. 1 Simple traffic network

In the literature [20]-[25], the fluid dynamic model is used to minimize the queue length at each link $l \in \mathcal{L}$. It simply represents the length $q_l(t)$ at time t which is the difference between the arrival rate evaluated at $\tilde{a}_l(t)$ and the departure rate evaluated at the same time t $d_l(t)$. Let's consider at red and green intervals, the departure and arrivals rate functions form an area bounded at each cycle time. These areas are calculated mathematically by using definite integrals under which lower and upper bounds represent the start of the red interval and the start of the green interval. The last upper bound is the cycle end which is considered to be 1. The uniform delay is the positive value of the differences in the areas for the red and the green intervals for each cycle. Since the arrival and departure are sinusoidal periodic functions of time, the uniform delay is periodic at each cycle. The arrivals rate pattern is assumed to be a uniform sinusoidal function. This could make it possible to approximate delays as a function of offsets. The concept to calculate the delay, in this case, it is the area bounded between the arrival and departure rates over a time scale.

Vehicles are permitted to pass through an intersection when the green signal is activated. To avoid traffic accidents, the conflict traffic movements are separated by activating different green time for each phase. A sequence of signals is generated to control the non-conflict traffic pattern. The optimization procedure is mainly used to optimize the cycle and the green time. The optimized values of cycle time are applied for the non-entry links whereas the entry links use the optimized cycle time for the whole signalized intersections. Fixed time control with a common cycle time is assumed for the signalized

network. This means that $C = 1$ for all intersection controlled with traffic signal at fixed periodic cycle, and all intersections have in common cycle time. It is divided into two intervals red and green. All intersections $w \in W$ obey to the signal offset $\theta \in [0,1)$, it is defined as the phase difference of the signal control sequence form the global clock. The vehicles are allowed to pass through downstream intersection $\sigma(l)$ at for each link $l \in \mathcal{L}$, thereby $n + \theta_{\sigma(l)} + \gamma_l$ for $n = 1,2,3$. The green split is represented by $\gamma_l \in [0,1)$, and it is the time of the ratio of effective green to the effective red of the downstream offset $\theta_{\sigma(l)}$. The offsets of the dummy links are taken to be zero due to the absents of upstream offsets at the entry links.

A. Sinusoidal Function Approximations

The departure rate is calculated by considering the flow (vehicles per hour) multiplied by the cycles of the effective green time as in (1). The results would be the number of vehicles leaving the intersection. The calculation procedure is provided below.

The estimation equation for the departures is:

$$d_l = s_l \left(\frac{veh}{sec}\right) * g_l(\text{sec}) \tag{1}$$

where d_l is the departure rate at link l (vehicle); s_l is the saturation flow rate at link l; g_l is the effective green time at link l (second).

Similar to [21], it is assumed that the network is in the periodic steady-state and we approximate all the arrivals and departures by sinusoidal functions with period $C = 1$. Especially, the departures rate of link l is assumed to be: -

$$\tilde{d}_l(t) = d_l + d_l \cos\left(2\pi\left(t - \theta_{\sigma(l)} - \gamma_l\right)\right) \tag{2}$$

where d_l is the average departure rate in vehicles for link l. The cosine is decomposed and written using the Euler identity and phasors. The definition becomes $z_j = \exp(i2\pi\theta_w)$ for $j \in W$ and $D_l = d_l \exp(-i2\pi\gamma_l)$, γ_l is the green split one can write the departure rate at link l as

$$\tilde{d}_l(t) = d_l + Re(\exp(i2\pi t) D_l z_{\sigma(l)}) \tag{3}$$

The arrival rate is calculated by considering the flow (vehicle per hour) times the cycle length. The results would be in vehicles. The calculations would be as follow:

$$f_l = q_l \left(\frac{veh}{sec}\right) * C_l\,(sec) \tag{4}$$

where:

$$f_l : the\ avarage\ arrival\ rate\ at\ link\ l\ (vehicle)$$
$$q_l : the\ flow\ at\ the\ entry\ link\ l\ (\tfrac{veh}{h})/3600$$
$$C_l : the\ cycle\ length\ at\ link\ l\ (second)$$

Vehicles arrive at a non-entry link from its upstream links after a uniform delay at the arrivals and departure vehicles, the arrival rate can be further expressed using Euler Identity and phasors as

$$\tilde{a}_l(t) = f_l + Re\{\exp(i2\pi t) A_l z_{\tau(l)}\} \tag{5}$$

where $A_l = \exp(-i2\pi\lambda_l), \lambda_l \in [1,0)$ it is held fixed and is taken to be 0,5 vehicles arrived at the non-entry links. For an entry link $l \in \mathcal{E}$, the approximation assumes that

$$\tilde{a}_l(t) = f_l + \alpha_l \cos\big(2\pi(t - \phi_l)\big) \tag{6}$$

$$= f_l + Re\big\{\exp(i2\pi t)\, A_l z_{\tau(l)}\big\} \tag{7}$$

where $z_{\tau(l)} = \exp(i2\pi\theta_n) = 1$ with the offset θ_n of the dummy intersection ϵ (intersection index n) defined to be 0 in (7), $\alpha_l \leq f_l$ is the relative amplitude of the arrival peak minus the average arrivals rate, $A_l = \alpha_l \exp(-2\pi\varphi_l)$, and $\varphi \in [0,1)$ is the offset for the center of the peak arrival, at the entry links φ is optimized in the non-entry links is taken to be 0,5. α_l is the fluctuation in the arrivals rate which is taken to be 50% of the arrivals rate f_l.

B. Uniform Delay and Offset Variable Relationship

The first part of this study is to formulate the cost function of uniform delay (UD_l). The vehicles arrived at the entry link ϵ. Since there is no upstream junction at the entry links, they are controlled by signalized downstream intersections $\sigma(l)$ located at the end of each entry link. These types of links control the amount of traffic demand entering the network through upstream intersections $\tau(l)$ located at the beginning of the non-entry links. Understandably, the downstream intersection for the entry links ϵ becomes the upstream intersection for the non-entry links. note that there is no upstream intersection for the entry links $\mathcal{E}$. The downstream junctions also would be the upstream intersections denoted by $\tau(l)$ for the non-entry links. Fig. 1 shows the possible traffic directions, thereby each signalized intersection works either with downstream for entry links or upstream for the non-entry links. These movements are considered the sinusoidal periodic function of time. There will be a uniform time lost in seconds at each intersection w per cycle C represented by the area-bounded (formed) between the arrival and departure rates. This representation is mathematically addressed the sinusoidal functions as it was mentioned in the previous section.

The cycle length is divided into two intervals effective red r (seconds) and effective green g (seconds) as it can be seen from Fig. 2. The uniform delay representation is the sinusoidal arrivals and sinusoidal departure rate functions at the green and red intervals forming an area between the arrivals and departure curves. The vehicles join the queue in for both the entry links (feeders) and the non-entry links at the red indication while the green indication where the vehicles are permitted to move to clears the signalized intersection. The concept is the difference of the summation of the areas bounded between $\tilde{a}_l(t)$ & $\tilde{d}_l(t)$ during the effective red period and the summation of the areas bounded between $\tilde{a}_l(t)$ & $\tilde{d}_l(t)$ during the effective green period. The area is calculated using the definite integration for one cycle. The concept is shown in:

$$UD_l = |Areas\ under\ red\ interval - Areas\ under\ green\ interval|$$

The offset included in the two periodic functions is a variable called the phase shift. The time lead and lag of the functions will cause the area to shrink and expand based on the offset selection (phase shift value). Moreover, the arrival offset value is the upstream interval of $\theta_{\tau(l)} \in [0,1)$ of the cycle time. The upstream offset value is adjusted by the center of peak arrival offset φ. On the other hand, the departure offset at the downstream intersection is adjusted according to the interval of $\theta_{\sigma(l)} \in [0,1)$ of the cycle time. The downstream offset is adjusted by portion of green split $\gamma_l \in [0,1)$ for adjusting the platoon movement at each intersection which is obviously seen at (2) & (6).

The upstream and downstream offsets with green split belong to the interval [0,1), this makes it difficult to solve the area-bounded between these sinusoidal functions. One can consider an example to visualize the scenario as in Fig. 2.

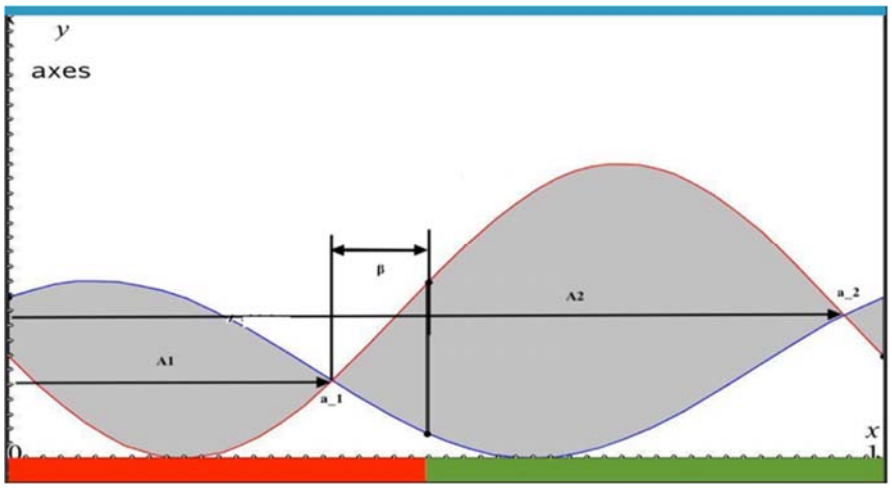

Fig. 2 Example of the periodic arrivals and departures rates bounded area per cycle

As indicated in Fig. 2, there are four terms for area-bounded per cycle $C = 1$. Our hypothesis of the delay here is the area bound of these sinusoidal periodic functions. The upper and the lower bounds for each antiderivative term are divided into four areas. The uniform delay represents the difference in the summation of the areas under the effective red and effective green as it is shown in (8):

$$UD_l = \int_0^{a_1} \tilde{a}(t) - \tilde{d}(t)dt + \int_{a_1}^{\beta} \tilde{d}(t) - \tilde{a}(t)dt - \left(\int_{\beta}^{a_2} \tilde{d}(t) - \tilde{a}(t)dt + \int_{a_2}^{1} \tilde{a}(t) - \tilde{d}(t)dt\right) \quad (8)$$

Equation (8) requires integration over four terms. The first term is integrated over the period from zero as a lower bound to the first intersection point over time corresponding to the x-axis at the upper bound denoted by a_1. The second area-bound corresponds to the period of a_1 to β. The third term integrated over the period β to a_2 because we assumed the cyclic period is 1. The integration bounds for the last integral are a_2 to 1. There are two intersection points a_1 and a_2, so how could we integrate over two unknown periods? The answer is at any scenario of different offsets in both arrival and departure rates and green split in both equations, the phase difference between $a_1$and a_2 is 0.5. So, we could substitute $a_2 = a_1 + 0.5$ which makes it easy to get rid of a_2 . To find a_1, refer to Section VI. The integration of (8) could be easy to compute. Thus, (8) becomes:

$$UD_l = \int_0^{a_1} f_l + \alpha_l \exp(i2\pi t(t-\phi_l)) - \left(d_l + d_l \exp(i2\pi t(t-\psi_l))\right)dt + \int_{a_1}^{\beta} d_l + d_l \exp(i2\pi t(t-\psi_l)) - \left(f_l + \alpha_l \exp(i2\pi(t-\phi_l))\right)dt - \left(\int_{\beta}^{0.5+a_1} d_l + d_l \exp(i2\pi(t-\psi_l)) - (f_l + \alpha_l \exp(i2\pi(t-\phi_l))dt + \int_{0.5+a_1}^{1} f_l + \alpha_l(\exp(i2\pi(t-\phi_l)) - \left(d_l + d_l \exp(i2\pi(t-\psi_l))\right)\right) \quad (9)$$

$$UD_l = \int_0^{a_1} f_l + \alpha_l \exp(i2\pi(t-\phi_l)) - d_l - d_l \exp(i2\pi(t-\psi_l))\,dt + \int_{a_1}^{1-\gamma_l-a_1} d_l + d_l \exp(i2\pi(t-\psi_l)) - f_l - \alpha_l \exp(i2\pi(t-\phi_l))dt - \int_{1-\gamma_l-a_1}^{0.5+a_1} d_l + d_l \exp(i2\pi(t-\psi_l)) - f_l - \alpha_l \exp(i2\pi(t-\phi_l))dt + \int_{0.5+a_1}^{1} f_l + \alpha_l \exp(i2\pi(t-\phi_l)) - d_l - d_l \exp(i2\pi(t-\psi_l))dt \quad (10)$$

After evaluating the integration above, the UD_l would be:

$$\left.\begin{array}{c} 4f_l\, a_1\pi i + \alpha_l \exp(i2\pi(a_1-\phi_l)) - 4d_l a_1\pi i \\ -2d_l \exp(i2\pi(a_1-\psi_l)) \\ -\alpha_l \exp(-i2\pi\phi_l) \\ +d_l \exp(-i2\pi\psi_l) + 4d_l\pi i(1-\gamma_l-a_l) + \\ 2d_l \exp(i2\pi(1-\gamma_l-a_1-\psi_l)) \\ -4f_l\pi i(1-\gamma_l-a_1) \\ -2\alpha_l \exp(i2\pi(1-\gamma_l-a_1-\phi_l)) - 4d_l\pi i(0.5+a_1) - \\ 2d_l \exp(i2\pi(0.5+a_1-\psi_l)) + \\ 4f_l i\pi(0.5+a_1) + 2\alpha_l \exp(i2\pi(0.5+a_1-\phi_l)) - 2\pi f_l i \\ -\alpha_l \exp(i2\pi(1-\phi_l) + 2\pi d_l i + d_l \exp(i2\pi(1-\psi_l)) \end{array}\right\rangle 2\pi i \quad (11)$$

C. The Procedure to Find the Intersection Point a_1

Fig. 3 shows how the intersection points $a_1$and a_2 are correlated geometrically. The intersect point a_1 has a big role in changing the UD_l (area-bounded). In other words, when the

offsets and the green split are optimized, a_1 shows noticeable shifting along the x-axis (time cycle which is taken to be one).

Based on the objective function, $a_1$is the arctangent of the area under the curve. The solution for a_1 is using the cosine identity decomposition. If we let $a_1 \in [\frac{-\pi}{2}, \frac{\pi}{2}]$, this would allow us to take all the possible scenarios when UD_l area is formed based on the offset values in both upstream and downstream intersections, and the green split at the downstream intersection. In between this interval, we would have various delay areas in which we could optimize the offsets to attain minimized delay for the traffic network.

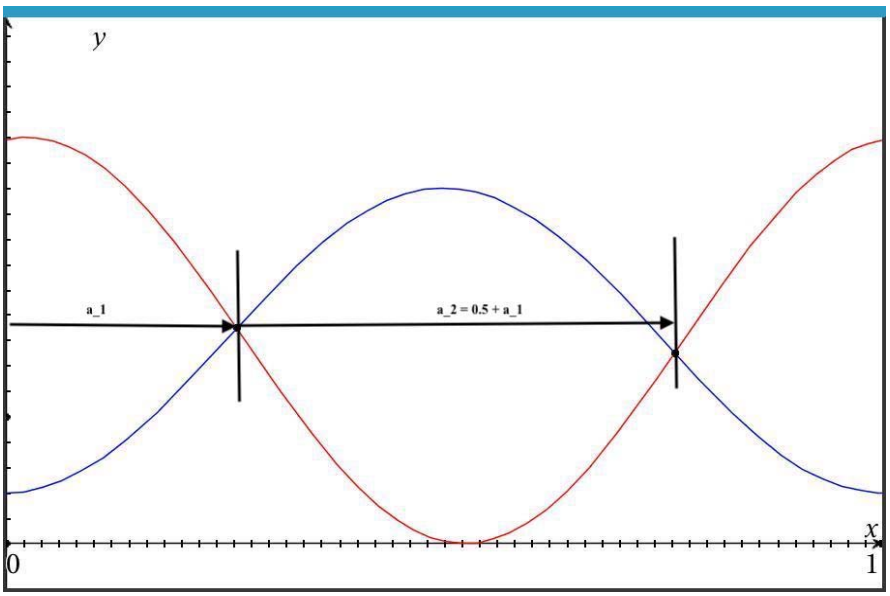

Fig. 3 The intersect points $a_1 and\ a_2$

The intersection point a_1 is where the two sinusoidal curves are equal in terms of values. Mathematically, we could equate the two functions to solve for a_1. Suppose we have two sinusoidal functions F_1 & F_2. These functions represent the arrival and departure rates under sinusoidal periodic. In non-simplified form cosine identities.

$$\tilde{a}_l(t) = \tilde{d}_l(t) = a_1 = F_1 \quad (12)$$

$$\tilde{a}_l(t) = \tilde{d}_l(t) = a_2 = F_2 \quad (13)$$

$$F_1 = \alpha_l \cos(2\pi a_1 - 2\pi\phi_l) \quad (14)$$

$$F_2 = f_l \cos(2\pi a_1 - 2\pi\psi_l) \quad (15)$$

Let $F_1 = F_2$ at point a_1, then we would have:

$$\alpha_l \cos(2\pi a_1 - 2\pi\phi_l) = f_l \cos(2\pi a_1 - 2\pi\psi_l) \quad (16)$$

By using the cosine identity, we decompose the right-hand side term, then we would have:

$$\alpha_l \cos(2\pi a_1 - 2\pi\phi_l) = f_l cos2\pi a_1 cos2\pi\psi_l + f_l sin2\pi a_1 sin2\pi\psi_l \quad (17)$$

Dividing both sides by $cos2\pi a_1$we obtain:

$$\frac{\alpha_l \cos(2\pi a_1 - 2\pi\phi_l)}{cos2\pi a_1} = f_l cos2\pi\psi_l + f_l tan2\pi a_1 sin2\pi\psi_l \quad (18)$$

To solve for a_1, we have:

$$tan2\pi a_1 = \frac{\alpha_l cos2\pi a_1 cos2\pi\phi_l + \alpha_l sin2\pi a_1 sin2\pi\phi_l}{f_l sin2\pi\psi_l cos2\pi a_1} - \frac{cos2\pi\psi_l}{sin2\pi\psi_l} \quad (19)$$

But we have:

$$tan2\pi a_1 = \frac{sin2\pi a_1}{cos2\pi a_1}$$

Then (19) becomes:

$$tan2\pi a_1 = \frac{\alpha_l cos2\pi\phi_l}{f_l sin2\pi\psi_l} + \frac{\alpha_l tan2\pi a_1 sin2\pi\phi_l}{f_l sin2\pi\psi_l} - \frac{cos2\pi\psi_l}{sin2\pi\psi_l} \quad (20)$$

Simplifying the terms above we get:

$$\frac{\alpha_l cos2\pi\phi_l}{f_l sin2\pi\psi_l} - \frac{cos2\pi\psi_l}{sin2\pi\psi_l} = tan2\pi a_1 - \frac{\alpha_l tan2\pi a_1 sin2\pi\phi_l}{f_l sin2\pi\psi_l} \quad (21)$$

Factoring out $tan2\pi a_1$from the right-hand side, we get:

$$\frac{\alpha_l cos2\pi\phi_l - f_l cos2\pi\psi_l}{f_l sin2\pi\psi_l} = tan2\pi a_1 \left(1 - \frac{\alpha_l sin2\pi\phi_l}{sin2\pi\psi_l}\right) \quad (22)$$

By doing more simplifications:

$$tan2\pi a_1 = \frac{\alpha_l cos2\pi\phi_l - f_l cos2\pi\psi_l}{f_l sin2\pi\psi_l - f_l \alpha_l sin2\pi\phi_l} \quad (23)$$

a_1 turns out to be the arctangent of the offset's differences between the upstream and downstream intersections:

$$a_1 = \frac{1}{2\pi} arctan\left(\frac{\alpha_l cos2\pi\phi_l - f_l cos2\pi\psi_l}{f_l sin2\pi\psi_l - f_l\alpha_l sin2\pi\phi_l}\right) \quad (24)$$

Note that

$$\phi_l = -(\varphi_{\tau(l)} + \theta_n),\ \ \psi_l = -(\theta_{\sigma(l)} + \gamma_l)$$

If we take the offsets to both be zero at the upstream and downstream intersections, in this case the arctangent argument is to infinity. Mathematically, this would not be a problem because the arctangent definition is the angle formed between the adjacent and the hypotenuse. When the adjacent approaches zero, the opposite will be large and form an angle belong to $\left[-\frac{\pi}{2}, \frac{\pi}{2}\right]$. If we would have a limit of a function that approaches infinity as shown in (25) and (26):

$$\lim_{n\to\infty}(\infty)^1 = \pi/2 \quad (25)$$

$$\lim_{n\to\infty}(-\infty)^1 = -\pi/2 \quad (26)$$

So, that makes it easy to let $a_1 \in [-\frac{\pi}{2}, \frac{\pi}{2}]$. In this case, a constraint is added to make the $a_1 \in [0, \frac{\pi}{2}]$, so, in this constraint we are forcing the a_1 to move around the first quadrant and calculate the possible areas based on the offset selection at each cycle. Since the cycle time is divided into two intervals red and green, the variable β is also important because alternating among the offset variable at both the upstream and the downstream intersections would change the interval from a_1 *to* β.

D.The Variable β

The variable β is either upper bound or lower bound for the definite integral to produce the area bounded between the arrival rate and departure rate. It is the distance from a_1 to the end of the red interval and the start of the green interval as indicated in Figs. 2 & 3. The procedure of calculating β is as follows: -

The green split is the ratio of the effective green to the cycle length:

$$\gamma_l = \frac{g}{C}, \gamma_l \in [0,1] \quad (27)$$

To find the effective red, (28) can be used:

$$r = 1 - \gamma_l \quad (28)$$

Since the $\gamma_l \in [0,1]$, the red time can be calculated in second as follows:

$$r = (1 - \gamma_l) * C \quad (29)$$

where the C is the cycle length, by using β definition and from Figs. 3 & 4, the β equation would be:

$$\beta = 1 - \gamma_l - a_1 \quad (30)$$

Neither γ_l nor a_1 values can be zero and β cannot be 1. Thus, the sum of γ_l and a_1 is negative and should not be bigger than 1 in magnitude; this would be the β value. This distance would be changed based on the offset's selection. The area bound between the arrivals and departure would change accordingly. The delay would change as well. The time lost between the two intervals is the uniform delay as it was explained earlier.

The final step of (11) for uniform delay UD_l and the objective function would be:

$$\left|\begin{array}{c} 12f_l\pi i - 12\, d_l\pi a_1 i + 4d_l\pi i - 4d_l\pi\gamma_l i + 4f_l\pi\gamma_l i - \\ 4f_l\pi\gamma_l i - P_l\left(\alpha_l\bar{z}_{\tau(l)}A_l - 2\alpha_l D_l\bar{z}_{\tau(l)}A_l + 2d_l D_l\bar{z}_{\sigma(l)}D_l\right)\Big/2\pi i \\ -\bar{z}_{\tau(l)}A_l - \alpha_l\bar{z}_{\tau(l)}A_l + 2d_l\bar{z}_{\sigma(l)}D_l \end{array}\right| \quad (31)$$

The scalers are removed because the algorithm optimizes the variables only. The final uniform delay objective function would be: -

$$\left|\begin{array}{c} f_l\pi i - d_l\pi a_1 i + d_l\pi i - d_l\pi\gamma_l i + f_l\pi\gamma_l i - \\ f_l\pi\gamma_l i - P_l\left(\alpha_l\bar{z}_{\tau(l)}A_l - 2\alpha_l D_l\bar{z}_{\tau(l)}A_l + 2d_l D_l\bar{z}_{\sigma(l)}D_l\right)\Big/2\pi i \\ -\bar{z}_{\tau(l)}A_l - \alpha_l\bar{z}_{\tau(l)}A_l + d_l\bar{z}_{\sigma(l)}D_l \end{array}\right| \quad (32)$$

subject to

$$\bar{z}_w = \exp(-i2\pi\theta_w), w = 1,2\ldots, n \quad (33)$$

$$P = \exp\left(-i \arctan\left(\frac{\alpha_l A_l\bar{z}_{\tau(l)} - f_l D_l\bar{z}_{\sigma(l)}}{B_l D_l\bar{z}_{\sigma(l)} - \alpha_l A_l B_l\bar{z}_{\tau(l)}}\right)\right), \in \left[0, \frac{\pi}{2}\right) \quad (34)$$

$$\gamma_l = \frac{g_l}{C_l} \in [0,1), g_l \in [30,90], C_l \in [120,180] \quad (35)$$

$$a_1 = \frac{1}{2\pi} * \arctan\left(\frac{\alpha_l A_l\bar{z}_{\tau(l)} - f_l D_l\bar{z}_{\sigma(l)}}{B_l D_l\bar{z}_{\sigma(l)} - \alpha_l A_l B_l\bar{z}_{\tau(l)}}\right) \quad (36)$$

The minimization objective function of UD_l uniform delay would be: -

$$\min_{\theta_w}\left|\begin{array}{c} f_l\pi i - d_l\pi a_1 i + d_l\pi i - d_l\pi\gamma_l i + f_l\pi\gamma_l i - f_l\pi\gamma_l i \\ -P_l\left(\alpha_l\bar{z}_{\tau(l)}A_l - 2\alpha_l D_l\bar{z}_{\tau(l)}A_l + 2d_l D_l\bar{z}_{\sigma(l)}D_l\right) \\ -\bar{z}_{\tau(l)}A_l - \alpha_l\bar{z}_{\tau(l)}A_l + d_l\bar{z}_{\sigma(l)}D_l \end{array}\Big/2\pi i\right| \quad (37)$$

subject to

$$\bar{z}_w = \exp(-i2\pi\theta_w),\ w = 1,2\ldots, n \quad (38)$$

$$P = \exp\left(-i \arctan\left(\frac{\alpha_l A_l\bar{z}_{\tau(l)} - f_l D_l\bar{z}_{\sigma(l)}}{B_l D_l\bar{z}_{\sigma(l)} - \alpha_l A_l B_l\bar{z}_{\tau(l)}}\right)\right), \in \left[0, \frac{\pi}{2}\right) \quad (39)$$

$$\gamma_l = \frac{g_l}{C_l} \in [0,1),\ \ g_l \in [30,90],\ \ C_l \in [120,180] \quad (40)$$

$$a_1 = \frac{1}{2\pi} * \arctan\left(\frac{\alpha_l A_l\bar{z}_{\tau(l)} - f_l D_l\bar{z}_{\sigma(l)}}{B_l D_l\bar{z}_{\sigma(l)} - \alpha_l A_l B_l\bar{z}_{\tau(l)}}\right), \in \left[0, \frac{\pi}{2}\right) \quad (41)$$

E. DE Optimization Algorithm

Metaheuristic algorithms show an efficient result to solve the traffic signal timing problems as it was presented in [5], [9], [28]. They are also simple and soft computational methods to implement and solve the nonlinear objective functions [35]. There is quite number of metaheuristic algorithms that could

solve the nonlinear optimization problems such as Ant Colony Optimization (ACO), GA, and Particle Swarm Optimization (PSO). However, recent studies [31], [36], [37] showed that the DE algorithm is a proper optimization tool for traffic signal timing which may reduce the total delay in signalized intersections. Furthermore, it is considered to be a powerful method to find the global optimal solution in a reasonable calculation time [31], [36], [37]. The estimation of average delay is investigated by comparing the results of two metaheuristics algorithms; genetic and DE [33]. The study shows that the DE algorithm presents the best convergence rate. The scope of this study is to derive a mathematical model for the uniform delay of the signalized network which is offset-dependent. The model is optimized by using the DE algorithm which is a simple, fast, and widely used technique to solve engineering problems [38]. It is a population-based metaheuristic algorithm as well as it is an improved version of the GA.

Reference [32] originally developed the Differential Evolution Algorithm (DEA), a simple and effective global optimization technique for solving continuous problems. It is a solid and robust algorithm and has had a good reputation owing to its superior performance in various engineering and scientific purposes since it was invented [39]. This algorithm is used to search for the global minimum for non-linear objective functions in (37). The basic DEA is used in this study which is mainly divided into four parts: initialization, mutation, crossover, and selection. The stopping criteria are also developed.

1) Initialization of First Population

$$x_{i,j,G=0} = rand[0,1]\left(x_j^H - x_j^L + 1\right) + x_j^L \quad i = \{1,2,3 \dots NP\}, j = \{1,2,3 \dots ND\} \tag{42}$$

First, the initial population needs to be created, (42). G is the number of generations; NP is the size of the population; ND is the number of decision variables; x_j^H, x_j^L maximum and minimum bounds of the j^{th} decision variables.

$$Population = \begin{bmatrix} C_1^1 & g_1^1 & \theta_1^1 & \theta_2^1 & \dots & \theta_{\mathcal{L}}^1 \\ C_1^2 & g_1^2 & \theta_1^2 & \theta_2^2 & \dots & \theta_{\mathcal{L}}^2 \\ \vdots & \vdots & \vdots & \vdots & \dots & \vdots \\ C_1^{NP} & g_1^{NP} & \theta_1^{NP} & \theta_2^{NP} & \dots & \theta_{\mathcal{L}}^{NP} \end{bmatrix} \rightarrow Fitness = \begin{bmatrix} (\sum_{l=1}^{\mathcal{L}} UD_l)^1 \\ (\sum_{l=1}^{\mathcal{L}} UD_l)^2 \\ \vdots \\ (\sum_{l=1}^{\mathcal{L}} UD_l)^{NP} \end{bmatrix}$$

2) Mutation

$$\mu_{i,j,G} = x_{r3,j,G} + F.\left(x_{r1,j,G} - x_{r2,j,G}\right) \tag{43}$$

The mutation operator in the DE strategy is applied to generate new mutated candidates to improve the solution. The commonly used mutation strategy $'DE/rand/1'$ was preferred in this study. F is the scaling coefficient; $r1, r2, r3$ are integer numbers randomly chosen among [1, NP] and cannot equal each other. If decision variables exceed lower or upper boundaries for any new candidate solution, they are reproduced again using (42). Summation of the uniform delay (UD_l) constitutes the objective function for each solution. According to the "Survival of Fittest" Principle, DEA's selection operators choose and transfer candidate solutions that minimize the total delay to the next generations. If a new mutation vector produces less delay, it will replace the previous generation, and this procedure continues until the stopping criteria are satisfied. There are 23 different upstream and downstream offsets (θ) that vary between [0,1] (7 entry links, 16 non-entry links). Other decision variables are Cycle (C) time and Effective green time (g).

3) Crossover

$$\gamma_{i,j,G} = \begin{cases} \mu_{i,j,G}, & \textbf{\textit{if }} rand(0,1) < CR \textbf{ \textit{or }} j = j_{rand} \\ x_{i,j,G}, & \textbf{\textit{otherwise}} \end{cases}$$

The diversity of the solution is tried to increase by selecting the genes from previous generations ($x_{i,j,G}$) and the mutant vector ($\mu_{i,j,G}$) with the crossover operator. CR is a real number ranging from [0-1]. The j_{rand} is added to ensure that at least one gene is retrieved from the mutant vector.

4) Selection

$$x_{i,j,G+1} = \begin{cases} \gamma_{i,j,G}, & \textbf{\textit{if }} \boldsymbol{f}(\gamma_{i,j,G}) < \boldsymbol{f}(x_{i,j,G}) \\ x_{i,j,G}, & \textbf{\textit{otherwise}} \end{cases}$$

The delays are calculated for the candidate mutant vector. If the delays are lesser than those obtained with the previous, the new solution is replaced with the old one in the selection operator.

5) Stopping Criteria

Optimization with DEA continues until the desired stopping criterion is satisfied. The tolerance value of the standard deviation of the fitness values or maximum simulation number can be chosen as the stopping criteria. In this study, the algorithm was stopped when the standard deviation (σ) of the Fitness matrix (F) became smaller than the $\varepsilon_{tol} = 0.001$. Fig. 5 shows a flowchart of the overall algorithm.

$$\sigma < \varepsilon_{tol}$$

$$\bar{f} = \frac{1}{NP}\sum_{i=1}^{NP} f^i \ , \ \sigma = \sqrt{\frac{1}{NP}\sum_{i=1}^{NP}(f^i - \bar{f})^2}$$

F. Case Study

A case study is chosen from the literature. The selected case was conducted by [34]. The network consists of seven zones and 23 links. We divided the links of the network into entry and non-entry links. Origin-destination zones are (A, D & E) while the other zones are either origin like (G & C) or destination like (B & F). The traffic movements among the zones are controlled by six signalized junctions to avoid collision. The network contains 23 links, and this study divided the links into two types. The entry links are denoted by $\epsilon \in \mathcal{L}$ and non-entry links are denoted by $\ell \in \mathcal{L}$ where $\mathcal{L}$ is the set of all links. The

signalized network could handle a demand between (1500 vehicles/hour – 3000 vehicles/hour). The network description is in Figs. 5 & 6. The first one shows the network layout which contains zones, links, and signalized intersections. The second one contains the traffic assignment and the traffic movements among the nodes and links. Each link has an upstream intersection denoted as $\tau(l)$ and the downstream intersection denoted by $\sigma(l)$. This is used to calculate the delay at each link by tuning up the offsets at the upstream $\theta_{\tau(l)}$ and the offset at the downstream $\theta_{\sigma(l)}$. Fig. 6 shows the possible stages for each signalized intersection.

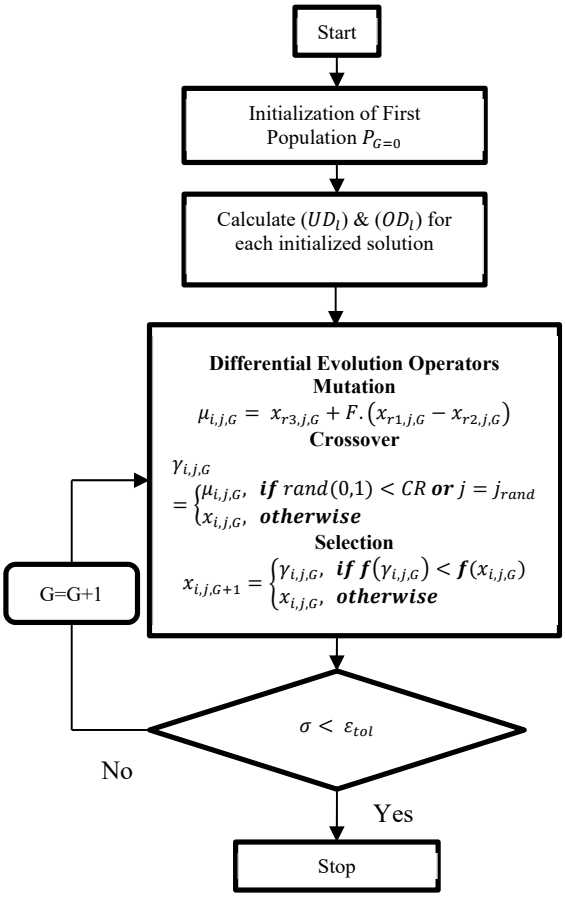

Fig. 4 Flowchart of DEA

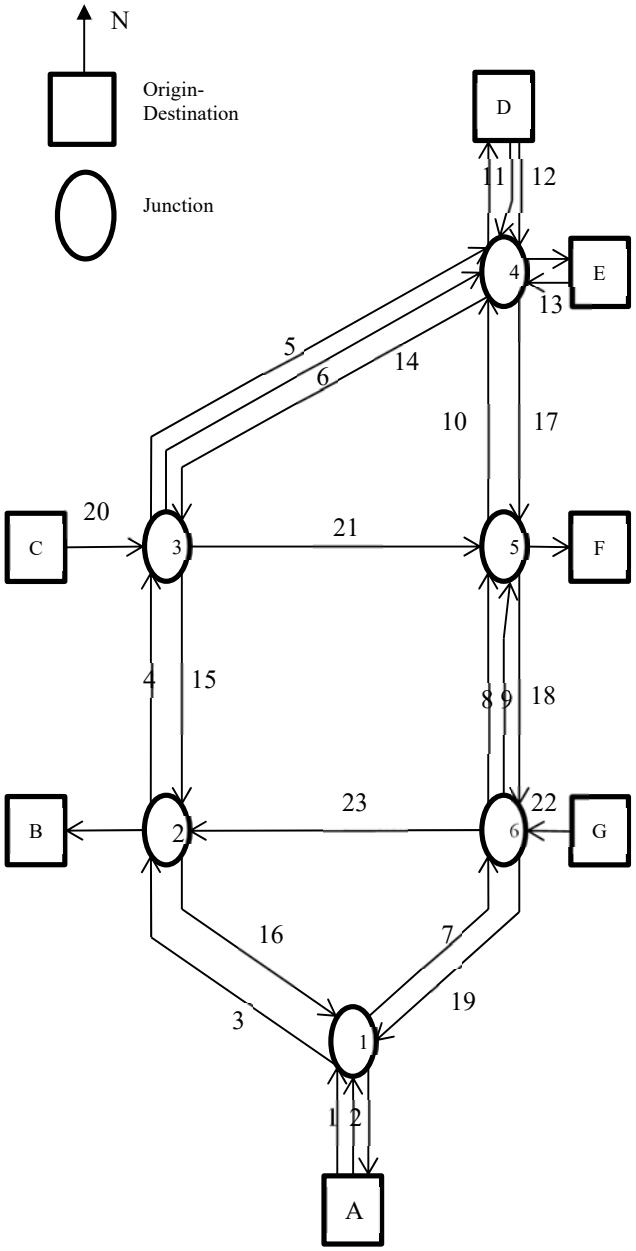

Fig. 5 The traffic network [34]

G. The Data Input for Optimizing the Network

The traffic flow at each link needs to be calculated for each link. It can be proposed when the traffic demand (arrival rate at each link) increases, we expect the highest delay value based on the link direction within the network and the path for each movement.

Table II shows the origin-destination matrix for the network in vehicles per hour. However, based on the uniform delay model, the average arrival rate is needed at each entry and non-entry link $\mathcal{E}, \ell \in \mathcal{L}$ where $\mathcal{L}$ is the set of all links in the network. Table III shows the saturation flow rates for the entry and non-entry links. Table IV reveals all the possible movements within the network. In other words, the path required is based on the driver's choice to travel between two zones of origin-destination. The first column in Table IV is for the origin-destination trips between zones. The second column is for the path approached from the origin zone to the destination zone. The third column is the percentage of traffic demand estimated to approach a specific path or movement. This is assumed randomly based on which movement has the smaller number of

signalized junctions fall into a specific path. This gives the highest percentage of traffic demand. The other paths are given a less percentage of traffic demand since the number of signalized junctions are higher than the other ones. The user choice is signalized traffic junction dependent. In other words, the best option for the user choice is the path that has the less signalized traffic junction. Otherwise, the trip was conducted on purpose which is considered less likely to happen. The data provided in Table II are used to calculate the traffic flow per path in vehicle per hour which is located in the fourth column of Table IV. The average arrival rate is the number of cars requesting a trip at each link denoted by f_l.

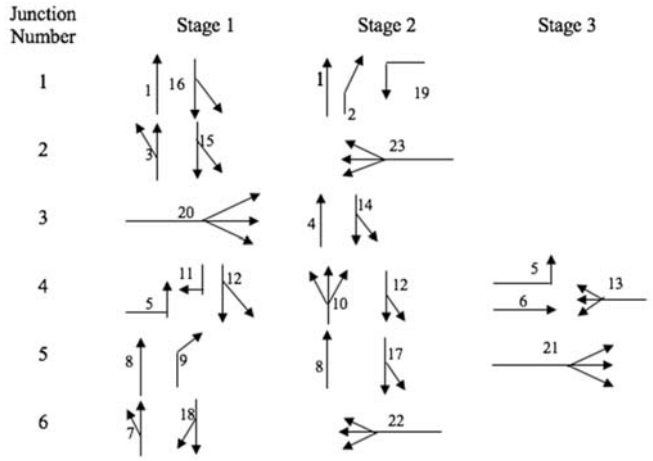

Fig. 6 The stages at each signalized intersection

It is worth mentioning that each intersection is given a specific color, the links connected to these intersections are given the same color as the junction is connected. The fluctuation of the arrival rate is denoted as $\alpha_l \leq f_l$. This value is held fixed for all the links which are to be 50% of the arrival rate for the undersaturated condition.

TABLE II
THE ORIGIN-DESTINATION MATRIX FOR THE NETWORK IN VEHICLE/HOUR.

Origin/Destination	A	B	D	E	F	Origin Totals
A	--	250	700	30	200	1180
C	40	20	200	130	900	1290
D	400	250	--	50*	100	800
E	300	130	30*	--	20	480
G	550	450	170	60	20	1250
Destination Totals	1290	1100	1100	270	1240	5000

*Where the travel demand between O-D pair D and E are not included in this numerical test which can be allocated directly via links 12 and 13.

The entry links are 7 (1, 2, 11, 12, 13, 20, 22). Then $\alpha_l = 0 \; \forall \; \ell \in \mathcal{E}$, and clearly, there is not any fluctuation in the arrival rate at the entry links. It is important to consider the offsets at the entry links are zero, so, $\bar{z}_{\tau(l)} = 1$ as an upstream offset. The downstream offset is varied (variable) and the downstream offsets are calculated first for all junctions and optimized. The calculated downstream offsets would be the upstream offsets for all the non-entry links. The non-entry links are 16, 3, 4, 5, 6, 7, 8, 9, 10, 14, 15, 16, 17, 18, 19, 21, 23.

TABLE III
THE SATURATED FLOW RATE FOR ENTRY AND NON-ENTRY LINKS

Junction number	Link	Saturated flow (veh/h)
1	1	2000
	2	1600
	16	2900
	19	1500
2	3	3200
	15	2600
	23	3200
3	4	3200
	14	3200
	20	2800
4	5	1800
	6	1850
	10	2200
	11	2000
	12	1800
	13	2200
5	8	1850
	9	1700
	17	1700
	21	3200
6	7	1800
	18	1700
	22	3600

H. Optimization Procedure

The metaheuristic approach is called DEA to optimize the objective function in (35) for the traffic network. The cycle time, effective green, the upstream and downstream offsets, and the offset at the center arrival rate for the entry links are optimized. The traffic signal network is divided into entry links where the cars enter the network and non-entry links which links the signalized junctions within the network. The optimization procedure is divided into two stages. In the first stage, the main difference between both groups is the upstream offsets $\theta_{\tau(l)}$ for the entry links are all zero. This is due to the connection of the entry links to dummy links. In this case, the offsets at the downstream junction $\theta_{\sigma(l)}$ (where the traffic signal is found) and the offsets of the periodic arrival $\varphi_{(\epsilon)}$ of vehicles to the queue of the entry link ϵ are considered variables.

Since the offset variable is responsible for synchronizing the traffic stream in the signalized network, the knowledge of the downstream offset for the entry links is important for upstream offsets of the non-entry links offsets. The offsets at the downstream junction $\theta_{\sigma(l)}$, and the offsets of the periodic arrival at the center of the entry links $\varphi_{(\epsilon)}$ are optimized with the cycle time and effective green time. These parameters are considered to be decision variables. The uniform delay is the measured parameter for the offsets. The decision variables are optimized to give the minimized uniform delay UD_l value for the entry links. The downstream offsets for the entry links are taken to be the upstream offsets for the non-entry links. Based on these values, the whole non-entry links offsets are optimized. The objective is to minimize the uniform delay at each link with the collection of offsets at the upstream and the downstream. The needed offsets are downstream which is considered in the

calculation.

TABLE IV
THE POSSIBLE MOVEMENTS AND TRAFFIC FLOW (VEH/H) PER PATH

Origin/ destination	User Path (Link Numbers)	Percentage of traffic demand (%)	Traffic Flow per path (veh/h)
A – B	3	100%	250
A – D	1, 3, 4, 5	26%	182
	1, 3, 4, 21, 10	7%	49
	2, 7, 8, 10	33%	231
	2, 7, 23, 4, 5	18%	126
	2, 7, 23, 4, 21, 10	16%	112
A – E	1, 3, 4, 6	20%	6
	1, 3, 4, 21, 10	22%	7
	2, 7, 8, 10	41%	12
	2, 7, 23, 4, 6	12%	4
	2, 7, 23, 4, 21, 10	5%	1.5
A – F	1, 3, 4, 21	23%	46
	2, 7, 9	59%	118
	2, 7, 23, 4, 21	18%	36
C – A	20, 15, 16	80%	32
	20, 21, 18, 19	20%	8
C – B	20, 15	85%	17
	20, 21, 18, 23	15%	3
C – D	20, 5	88%	176
	20, 21, 10	7%	14
	20, 15, 16, 7, 8, 10	5%	10
C – E	20, 6	89%	116
	20, 21, 10	8%	10
	20, 15, 16, 7, 8, 10	3%	4
C – F	20, 21	92%	828
	20, 15, 16, 7, 9	8%	72
D – A	12, 17, 18, 19	46%	184
	11, 14, 15, 16	23%	92
	11, 14, 21, 18, 19	10%	40
	12, 17, 18, 23, 16	16%	64
	11, 14, 21, 18, 23, 16	5%	20
D – B	11, 14, 15	73%	183
	12, 17, 18, 23	17%	43
	11, 14, 21, 18, 23	10%	25
D – E	12	100%	50
D – F	12, 17	86%	86
	11, 14, 21	10%	10
	11, 14, 15, 16, 7, 9	4%	4
E – A	13, 17, 18, 19	32%	96
	13, 14, 15, 16	25%	75
	13, 14, 21, 18, 19	17%	51
	13, 17, 18, 23, 16	16%	48
	13, 14, 21, 18, 23, 16	10%	30
E – B	13, 14, 15	52%	68
	13, 17, 18, 23	40%	52
	13, 14, 21, 18, 23	8%	10.4
E-D	13	100%	30
E – F	13, 17	88%	18
	13, 14, 21	10%	2
	13, 14, 15, 16, 7, 9	2%	1
G – A	22, 19	80%	440
	22, 23, 16	10%	55
	22, 8, 10, 14, 15, 16	5%	28
	22, 8, 10, 14, 21, 18, 19	4%	22
	22, 8, 10, 14, 21, 18, 23, 16	1%	5.5
G – B	22, 23	94%	423
	22, 8, 10, 14, 15	6%	27
G – D	22, 8, 10	95%	162
	22, 23, 4, 5	5%	8.5
G – E	22, 8, 10	91%	55
	22, 23, 4, 6	6%	4
	22, 23, 4, 21, 10	3%	2
G – F	22, 9	96%	19
	22, 23, 4, 21	4%	1

Note: - The Red color for junction 1. The Yellow color for junction 2. The Black color for junction 3. The Green color for junction 4. The Blue color for junction 5. The Brown color for junction 6.

The center offset of the arrival peak at the non-entry links $\varphi_{(l)}$ is taken to be a fixed value equal to 0.5. The fluctuation α_l in the arrivals rates is considered to be 50% of the arrivals flow rate value f_l.

III. RESULTS

The uniform delay is calculated based on Webster's first term and [40]; results are shown in Table V. These models are quite acceptable and recognized in academic research. The Webster's uniform delay results are shown in the third column. In the fourth and fifth columns, the study generates the new uniform delay and highway capacity manual HCM uniform delay models respectively. The upstream and downstream offsets are in columns eighth and ninth. The degree of saturation is in the tenth column.

As it can be seen from Table V, the entry links 2, 22, and 20 have delay 33 seconds for Webster's uniform delay while 31 seconds for HCM uniform delay model. Based on the new model, the entry links mentioned earlier have uniform delays of 5, 10, and 10 seconds respectively. Although the degree of saturation indicates their condition of congestion, the non-links uniform delay values ranged from 22-30 seconds for the Webster model and 21-29 seconds for HCM. On the other hand, the new uniform delay model results range 4-24. The total uniform delays for Webster model, HCM model and the new derived model are 674 sec, 638 sec, and 360 sec, respectively.

The uniform delay offset model results are shown in Tables VI and VII. As it was mentioned in the theory part, each entry link has a downstream offset. The knowledge of the downstream offset at the entry links is important to the upstream offsets for the non-entry links. Accordingly, the downstream offsets at each link should be considered as a final coordination value in seconds. However, at each signalized junction, the number of stages is 2-3 according to the junction position in the network, each stage consists of at least 1 to 3 links, refer to Fig. 6. The downstream offsets are selected based on which link has got the highest offset value as it is seen in Table VI and the lowest offset value as seen in Table VII.

IV. DISCUSSION

The uniform delay for Webster and HCM is compared to the model derived in this study. In the previous section, the nonrandom delay for the two comparable models is almost the same with minor differences of around 36 seconds less for HCM. To show the robustness of the model derived in this study, a comparison of the results is made. The total uniform delays for Webster, HCM and new derived models are 674 sec, 638 sec, and 360 sec, respectively. The new uniform delay is decreased almost to half of values in Webster and HCM models. This shows the efficiency of the derived model in the discission making of offset variables to minimize the uniform delay component for the signalized network. Linking the degree of saturation with Webster and HCM models showed no difference in uniform delay values because the uniform delay is countable to the saturation condition when $x = 1$. However, in the derived model, at each link, the uniform delay value is

decreased on one hand. On the other hand, the x values indicate oversaturation conditions on the links that experience higher demand. The case justification is that the derived model depends on periodic arrivals and departure while the other models depend either on Poison arrivals and departure rates.

TABLE V
ALL THE RESULTS VALUES AFTER OPTIMIZATION OF CYCLE TIME, UPSTREAM OFFSETS (SEC), AND DOWNSTREAM OFFSETS (SEC) TO MEASURE THE UNIFORM DELAY (SEC) WITH FLUCTUATION IN THE ARRIVALS RATE α_l= 50%, COMPARED WITH WEBSTER'S UNIFORM DELAY MODEL & HCM UNIFORM MODEL

Link no	Avg Arrival rate (veh/h)	Webster uniform delay (sec)	Uniform delay per link	HCM	Offsets		Cycle time (sec)	Upstream Offsets = $\theta_{\tau(l)} * cycle$	Downstream offsets = $\theta_{\sigma(l)} * cycle$	Degree of saturation (x)
1*	540	0	0	0	$\theta_{\tau(l)}$	$\theta_{\sigma(l)}$		0	0	0.95
2	640	33	5	31	0	0.81		0	86	1.4
22	1250	33	10	31	0	0.80		0	96	1.22
20	1290	33	10	31	0	0.80		0	96	1.62
13	480	29	5	28	0	0.81		0	91	0.77
11	374	27	4	26	0	0.81		0	86	0.66
12	427	30	4	29	0	0.81		0	86	0.83
3	540	26	14	25	0	0.83		0	86	0.59
16	539	27	13	26	0.12	0.80		13	86	0.65
7	731	33	25	31	0.81	0.84		86	89	1.43
19	833	33	28	31	0.80	0.84		86	86	1.96
4	547	26	13	25	0.12	0.80	106	13	89	0.60
15	611	30	21	28	0.80	0.83		86	89	0.83
23	1080	33	37	31	0.80	0.83		86	86	1.19
5	529	33	18	31	0.80	0.84		86	89	1.03
6	129	22	4	21	0.80	0.85		86	89	0.24
14	629	28	24	27	0.81	0.83		86	89	0.76
21	1333	33	45	31	0.80	0.83		86	95	1.47
17	590	33	20	31	0.81	0.84		86	89	1.22
10	751	33	17	31	0.12	0.80		13	89	1.20
18	701	33	16	31	0.12	0.81		13	89	1.45
8	555	33	19	31	0.80	0.84		86	86	1.06
9	214	33	8	31	0.80	0.87		86	86	1.07
Total Uniform delay (sec)		674	360	638	*Link 1 is always green. therefore, there is no delay or time lost noticed. Cars were directed to link 3.					

TABLE VI
THE HIGHEST DOWNSTREAM OFFSETS

Total uniform delay (sec)	Cycle time (sec)	Junction number	Offsets per stage		
			Stage 1	Stage 2	Stage 3
360	106	1	86	86	-
		2	89	86	-
		3	96	89	-
		4	89	89	91
		5	86	89	95
		6	89	96	-

TABLE VII
THE LOWEST DOWNSTREAM OFFSETS

Total uniform delay (sec)	Cycle time (sec)	Junction number	Offsets per stage		
			Stage 1	Stage 2	Stage 3
360	106	1	0	0	-
		2	86	86	-
		3	96	89	-
		4	86	86	89
		5	86	86	95
		6	89	96	-

Furthermore, the model successfully linked the offsets variable to uniform delay. The coordination values are recorded for each junction distributed at each stage in Tables VI and VII. The offset values are almost the same in both tables. The offset value is zero at junction 1 for stages 1 & 2 as it is seen in Table II. This is due to link 1 which is not controlled by the traffic light.

V. CONCLUSIONS

The direct relationship of the uniform delay and offset variable is derived using the DEA. The Webster's first term and HCM 2010 uniform delay models are used to compare with the derived uniform model which is basically the difference between the areas formed under the red and the green intervals. The derived model shows decreases in uniform delay value to almost half of that in the canonical uniform delay by Webster and HCM. The model shows that the uniform delay is offset-dependent. This may solve the coordination problem and minimizes the delay in large-scale signalized traffic networks.

REFERENCES

[1] F. v. Webster, "Traffic signal settings," *Road Research Technical Paper, No.39, Road Research Laboratory, London*, p. 44, 1958.
[2] W. Fawaz and J. El Khoury, "An exact modelling of the uniform control traffic delay in undersaturated signalized intersections," *Journal of Advanced Transportation*, vol. 50, no. 5, pp. 918–932, 2016, doi: 10.1002/atr.1387.
[3] N. Rouphail, A. Tarko, and J. Li, "Traffic flow at signalized intersections," in *Revised Monograph on Traffic Flow Theory*, 1992.
[4] S. W. Chiou, "TRANSYT derivatives for area traffic control optimisation

with network equilibrium flows," *Transportation Research Part B: Methodological*, vol. 37, no. 3, pp. 263–290, 2003, doi: 10.1016/S0191-2615(02)00013-9.

[5] Halim. Ceylan, "Developing combined genetic algorithm—Hill-climbing optimization method for area traffic control," *Journal of Transportation Engineering*, vol. 132, no. 8, pp. 663–671, Aug. 2006, doi: 10.1061/(ASCE)0733-947X (2006)132:8(663).

[6] S. W. Chiou, "An efficient algorithm for optimal design of area traffic control with network flows," *Applied Mathematical Modelling*, vol. 33, no. 6, pp. 2710–2722, 2009, doi: 10.1016/j.apm.2008.08.009.

[7] S. W. Chiou, "A novel algorithm for area traffic capacity control with elastic travel demands," *Applied Mathematical Modelling*, vol. 35, no. 2, pp. 650–666, 2011, doi: 10.1016/j.apm.2010.07.016.

[8] S. W. Chiou, "Optimization of robust area traffic control with equilibrium flow under demand uncertainty," *Computers & operations, Elsevier*, vol. 41, pp. 399–411, Jan. 2014.

[9] Halim. Ceylan, "A genetic algorithm approach to the equilibrium network design problem.," University of Newcastle upon Tyne, 2002.

[10] R. E. Allsop, "Delay-minimizing settings for fixed-time traffic signals at a single road junction," *IMA Journal of Applied Mathematics (Institute of Mathematics and Its Applications)*, vol. 8, no. 2, pp. 164–185, Oct. 1971, doi: 10.1093/imamat/8.2.164.

[11] R. E. Allsop, "Delay at a fixed time traffic signal--1. theoretical analysis" *Transportation Science*, vol. 6, no. 3, pp. 260–285, 1972, doi: 10.1287/TRSC.6.3.260.

[12] G. Improta and G. E. Cantarella, "Control system design for an individual signalized junction," *Transportation Research Part B*, vol. 18, no. 2, pp. 147–167, 1984, doi: 10.1016/0191-2615(84)90028-6.

[13] B. Heydecker and I. Dudgeon, "Calculation of signal settings to minimise delay at a junction," *Transportation and Traffic Theory*, 1987.

[14] A. Muralidharan, R. Pedarsani, and P. Varaiya, "Analysis of fixed-time control," *Transportation Research Part B: Methodological*, vol. 73, pp. 81–90, Mar. 2015, doi: 10.1016/J.TRB.2014.12.002.

[15] G. Improta and A. Sforza, "Optimal offsets for traffic signal systems in urban networks," *Transportation Research Part B: Methodological*, vol. 16, no. 2, pp. 143–161, Apr. 1982, doi: 10.1016/0191-2615(82)90032-7.

[16] G. E. Cantarella, G. Improta, and A. Sforza, "Iterative procedure for equilibrium network traffic signal setting," *Transportation Research Part A: General*, vol. 25, no. 5, pp. 241–249, Sep. 1991, doi: 10.1016/0191-2607(91)90141-C.

[17] J. A. Hillier and R. Rothery, "The Synchronization of Traffic Signals for Minimum Delay," *Transportation Science*, vol. 1, no. 2, pp. 81–94, 1967, doi: 10.1287/trsc.1.2.81.

[18] S. C. Wong, "Derivatives of the performance index for the traffic model from TRANSYT," *Transportation Research Part B*, vol. 29, no. 5, pp. 303–327, Oct. 1995, doi: 10.1016/0191-2615(95)00012-3.

[19] S. Lee, S. C. Wong, and P. Varaiya, "Group-based hierarchical adaptive traffic-signal control part I: Formulation," *Transportation Research Part B: Methodological*, vol. 105, pp. 1–18, 2017, doi: 10.1016/j.trb.2017.08.008.

[20] S. Coogan, G. Gomes, E. Kim, M. Arcak, and P. Varaiya, "Offset optimization for a network of signalized intersections via semidefinite relaxation," *Conference Publication IEEE*, 2015. https://ieeexplore.ieee.org/document/7402531 (accessed Jan. 26, 2022).

[21] S. Coogan, E. Kim, G. Gomes, M. Arcak, and P. Varaiya, "Offset optimization in signalized traffic networks via semidefinite relaxation," *Transportation Research Part B: Methodological*, vol. 100, pp. 82–92, Jun. 2017, doi: 10.1016/j.trb.2017.01.016.

[22] Z. Amini, S. Coogan, C. Flores, A. Skabardonis, and P. Varaiya, "Optimizing Offsets in Signalized Traffic Networks: A Case Study," *Conference on Control Technology and Applications (CCTA) IEEE*, Aug. 2018.

[23] E. S. Kim, C. J. Wu, R. Horowitz, and M. Arcak, "Offset optimization of signalized intersections via the Burer-Monteiro method," *Proceedings of the American Control Conference*, pp. 3554–3559, Jun. 2017, doi: 10.23919/ACC.2017.7963497.

[24] Y. Ouyang, R. Y. Zhang, J. Lavaei, and P. Varaiya, "Conic Approximation with Provable Guarantee for Traffic Signal Offset Optimization," *IEEE Conference on Decision and Control (CDC)*, pp. 229–236, Dec. 2018.

[25] Y. Ouyang, R. Y. Zhang, J. Lavaei, and P. Varaiya, "Large-Scale Traffic Signal Offset Optimization," *Transactions on Control of Network Systems IEEE,* vol. 7, no. 3, pp. 1176–1187, Sep. 2020, doi: 10.1109/TCNS.2020.2966588.

[26] N. H. Gartner, J. D. C. Little, and H. Gabbay, "Optimization of Traffic Signal Settings by Mixed-Integer Linear Programming - 1. the network coordination problem.," *Transportation Science*, vol. 9, no. n, pp. 321–343, Nov. 1975, doi: 10.1287/trsc.9.4.321.

[27] R. A. Vincent, A. I. Mitchell, and D. I. Robertson, "User Guide to Transyt Version 8," *Transport and Road Research Laboratory (TRRL) (No. LR 888 Monograph).*, p. 86, 1980.

[28] Halim. Ceylan and M. G. H. Bell, "Traffic signal timing optimisation based on genetic algorithm approach, including drivers' routing," *Transportation Research Part B: Methodological*, vol. 38, no. 4, pp. 329–342, 2004, doi: 10.1016/S0191-2615(03)00015-8.

[29] E. Almasri and B. Friedrich, "Online offset optimisation in urban networks based on cell transmission model," *Institute of Transport, Road Engineering and Planning University of Hannover, Appelstr. 9A, 30167 Hannover, Germany*, 2005.

[30] C. M. Day and D. M. Bullock, "Computational efficiency of alternative algorithms for arterial offset optimization," *Transportation Research Record*, no. 2259, pp. 37–47, 2011, doi: 10.3141/2259-04.

[31] H. Ceylan, "Optimal Design of Signal Controlled Road Networks Using Differential Evolution Optimization Algorithm," *Mathematical Problems in Engineering*, vol. 2013, p. 11, 2013, doi: 10.1155/2013/696374.

[32] R. Storn and K. Price, "Differential Evolution-A Simple and Efficient Heuristic for Global Optimization over Continuous Spaces," *Journal of Global Optimization*, vol. 11, pp. 341–359, 1997.

[33] S. S. Leal, P. E. M. De Almeida, and E. Chung, "Active control for traffic lights in regions and corridors: An approach based on evolutionary computation," *Transportation Research Procedia*, vol. 25, pp. 1769–1780, 2017, doi: 10.1016/j.trpro.2017.05.140.

[34] R. E. Allsop and J. A. Charlesworth, "Traffic in a Signal-Controlled Road Network: An Example of Different Signal Timings Including Different Routeing," *Traffic Engineering & Control*, vol. 18, no. 5, May 1977.

[35] M. Abdel-Basset, L. Abdel-Fatah, and A. K. Sangaiah, "Metaheuristic Algorithms: A Comprehensive Review," *Computational Intelligence for Multimedia Big Data on the Cloud with Engineering Applications*, pp. 185–231, Jan. 2018, doi: 10.1016/B978-0-12-813314-9.00010-4.

[36] Z. Cakici and Y. S. Murat, "A Differential Evolution Algorithm-Based Traffic Control Model for Signalized Intersections," *Advances in Civil Engineering*, p. 16, 2019, doi: 10.1155/2019/7360939.

[37] E. Korkmaz and AP Akgüngör, "Delay estimation models for signalized intersections using differential evolution algorithm," *Journal of Engineering Research*, vol. 5(3), pp. 16–29, 2017.

[38] R. Storn and K. Price, "Differential evolution - A simple and efficient adaptive scheme for global optimization over continuous spaces," 1995.

[39] K. V Price, R. M. Storn, and J. A. Lampinen, *Differential Evolution. A Practical Approach to Global Optimization*. 2005.

[40] Highway Capacity Manual, "Highway Capacity Manual 2010," Transportation Research Board, Washington, DC, 2, 1., Nov. 2010.